Journal of Alloys and Compounds 499 (2010) 206–211

Contents lists available at ScienceDirect

Journal of Alloys and Compounds

journal homepage: www.elsevier.com/locate/jallcom

Influence of hot-spot temperature on oxygen sensing response behavior of Er123 ceramic rods with hot spot

M. Hassan, A.K. Yahya*

School of Physics and Materials Studies, Faculty of Applied Sciences, Universiti Teknologi MARA, 40450 Shah Alam, Selangor, Malaysia

ARTICLE INFO

Article history:
Received 1 December 2009
Received in revised form 16 March 2010
Accepted 18 March 2010
Available online 25 March 2010

Keywords:
Er123
Hot spot
Oxygen sensor

ABSTRACT

Hot-spots appearing on several RE123 ceramics upon application of external voltage have been reported to show sensitivity towards different oxygen partial pressures. In this paper, influence of hot-spot temperature in the range of 160–810 °C on oxygen sensing behavior of Er123 sensor rods is reported. Simultaneous measurements of hot-spot temperature and output current response in different oxygen partial pressures between 1% and 100% showed hot-spots operating at temperatures as low as 660 °C in 1% oxygen partial pressure produced good stability and repeatability. Response time for oxygen sensing was observed to decrease with increasing hot-spot temperature, with minimum value of 0.50 s recorded at 695 °C in 1% oxygen partial pressure. In addition, a large change in activation energy from 2.8 eV to 0.626 eV was established at around 670 °C and this has been suggested to be related to structural change from orthorhombic to tetragonal taking place at around the same temperature. The reduction of activation energy increased diffusion of oxygen ions in the rod and caused rapid changes in resistivity which triggered movement of the hot spot to the negative electrode.

1. Introduction

The potential application of $GdBa_2Cu_3O_{7-\delta}$ (Gd123) ceramics utilizing hot spots as oxygen sensing elements was proposed quite recently [1,2]. Their suggestion follows earlier observations of formation of oxygen-sensitive hot-spots in RE123 (RE = Gd and Sm) ceramic rods [3]. Upon application of external voltage, the output current was observed to be sensitive to oxygen partial pressure, pO_2 and thus it was suggested as a potential candidate for oxygen sensing in ambient temperature. In contrast to most ambient oxygen sensors [4–9], the design of the hot-spot based sensors is in the form of a simple thin rod which can be easily fabricated and reproduced for large scale industrial applications. Besides being external-heater free, the sensor also uses a simple sensing system based on magnitude of output current.

RE123 (RE = Y and almost all rare earth elements) ceramics are of perovskite-type structure and is a well known oxygen deficient material. Their structure is orthorhombic at high oxygen content (low δ) and changes to tetragonal at low oxygen content (high δ). It was also known that at elevated temperatures, equilibrium oxygen content decreases with increasing temperature and decreasing pO_2 [10,11]. Well before the discovery of oxygen-sensitive hot spots, it was shown by Sageev Grader et al. [12] that hot-spot free Y123 gave some response to oxygen gas above 320 °C. Later, Takata et al. upon application of external voltage discovered hot spots in Gd123 and Sm123 rods at around 900 °C which showed sensitivity to oxygen gas. At the oxygen-sensitive hot spot, when the pO_2 is raised, the material absorbs oxygen which dissociates into holes and oxide ions. The net reaction involved during the absorption and desorption of oxygen gas is as follows:

$$O_2 \rightleftharpoons 2O'' + 4h^* \quad (1)$$

where O'' is an oxide ion and h^* is a hole. Oxygen absorption produces significant change in conductivity which was used for proposes of oxygen detection [3].

However, being a positive temperature coefficient of resistivity (PTCR)-based material, not only resistivity of the RE123 ceramic rod but also those of the hot spot are expected to increase with temperature [1]. In addition, oxygen absorption at the hot-spot area is also expected to be influenced by temperature as previous reports on resistivity [12] and thermogavimetry measurements [13] on hot-spot free Y123 reported strong influence of temperature on oxygen absorption and desorption rates. Previous studies on hot-spot free heated Y123 also reported change in activation energy of oxide ion migration upon reaching tetragonal phase from orthorhombic phase [14,15]. Based on these indications, behavior of the oxygen-sensitive hot spot is expected to be influenced by temperature and current–voltage characterization of the oxygen sensing behavior is not complete without monitoring temperature of the hot spot. However, such studies have not been previously reported.

* Corresponding author. Tel.: +60 355444613; fax: +60 355444562.
E-mail address: ahmad191@salam.uitm.edu.my (A.K. Yahya).

0925-8388/$ – see front matter © 2010 Elsevier B.V. All rights reserved.
doi:10.1016/j.jallcom.2010.03.167

Technically, one potential difficulty with the hot-spot based sensors that must be overcome before wider use of the sensor is related to the hot-spot temperature which was reported to reach as high as 940 °C [3]. This temperature is close to the melting temperature of RE123 materials and is detrimental to the durability of the sensor rods. One way to over come is by addition with secondary phase with higher melting temperature, such as $BaAlO_4$, however the addition caused reduction in sensor's sensitivity [16–18]. Therefore, understanding of temperature variation behavior of the hot-spot and its influence on oxygen sensing properties is of paramount importance as it may open up the possibility of operating the sensor at much lower temperatures to avoid breakage.

Recently, we have established oxygen sensing response of Er123 rods and observed excellent reproducibility and stability of output sensing current for pO_2 down to 0.025% [19]. In this paper, we further investigate the oxygen response behavior by studying the influence of hot-spot temperature on oxygen sensing. We report results of simultaneous observation of sensor output current and hot-spot temperature response with applied voltage for Er123 sensor rods at hot-spot temperatures in the range of 160–810 °C in 1% and 100% pO_2. Sensor response and recovery time behavior during alternating pO_2 between 1% and 100% are also reported. In addition, based on response time versus temperature data we report a change in oxide ion activation energy at 670 °C.

2. Experimental details

Bulk Er123 sample was synthesized from high purity (≥99.95%) Er_2O_3, $BaCO_3$ and CuO powders using conventional solid state reaction method. The appropriate amount of powders were mixed and ground in an agate mortar. The powders were then calcined in a box furnace at 900 °C for 48 h with several intermittent grindings. The powders were then reground and pressed into pellets and sintered at 900 °C for 24 h in a box furnace followed by slow cooling to room temperature. Powder X-ray Diffraction (XRD) analysis by Cu-K_α radiation using Rigaku model D/MAX 2000 PC was used to confirm the sample structure. The microstructure was observed under a LEO model 982 Gemini scanning electron microscope (SEM). Er123 sensor was fabricated by cutting the sample into rectangular rods with a fix dimension of 12 mm × 0.65 mm × 0.65 mm. For investigation of origin of hot spots a wider rectangular shape with a dimension of 12 mm × 4 mm × 0.65 mm was used. Electrical measurements were performed using a four-point-probe method with the distance between voltage electrodes being 9 mm. The voltage between the electrodes was supplied by an Agilent model 6575A current source. The current and voltage through the sensor were measured using Keithley multimeters models 2000 and 197A, respectively. *I–V* characterizations of the sensor before and after appearance of the hot spot were conducted in a chamber for 1% and 100% (1 atm) pO_2. The readings of the *I–V* characteristics in 100% and then 1% pO_2 were taken after the sensor has been exposed to the respective pO_2 during hot-spot appearance for more than 1 min. Oxygen sensing response was observed in a chamber which flows pure oxygen gas and 1% oxygen in nitrogen, alternately. The temperature of the sample was measured by IMPAC non-contact pyrometer model IP 140 which can detect temperature for spot size as low as 0.4 mm in the temperature range of 160 °C and 1200 °C with uncertainty between 2 °C and 5 °C, respectively.

3. Results and discussion

XRD pattern (figure not shown) of the synthesized Er123 powder showed formation of single phased 123 orthorhombic structure with space group *Pmmm*. The calculated lattice parameters *a*, *b* and *c* are 3.814 Å, 3.882 Å and 11.675 Å, respectively and the relative density is 72%. Fig. 1 shows SEM image of the internal section of the sample before (Fig. 1(a)) and after hot spot formation (Fig. 1(b)). Before hot spot formation, the microstructure showed irregular grains with size of 2–10 μm. After hot spot formation, the porosity increased and neck growth was observed between grains.

Fig. 2(a) and (b) shows sensor output current and temperature curves for the hot-spot area versus applied voltage across the rod in 1% and 100% pO_2, respectively. For applied voltage, *V* below 0.5 V, output current, *I* for both pO_2 showed a linear increase with voltage. With further increase in applied voltage, the slope of *I–V* curve begins to decrease until the output current reached a maximum

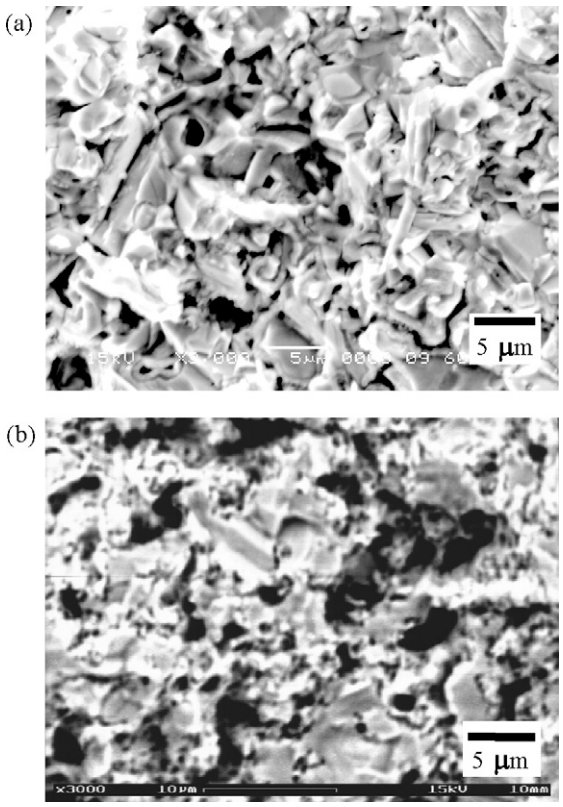

Fig. 1. SEM image of the internal section of the sample (a) before hot spot formation and (b) after hot spot formation.

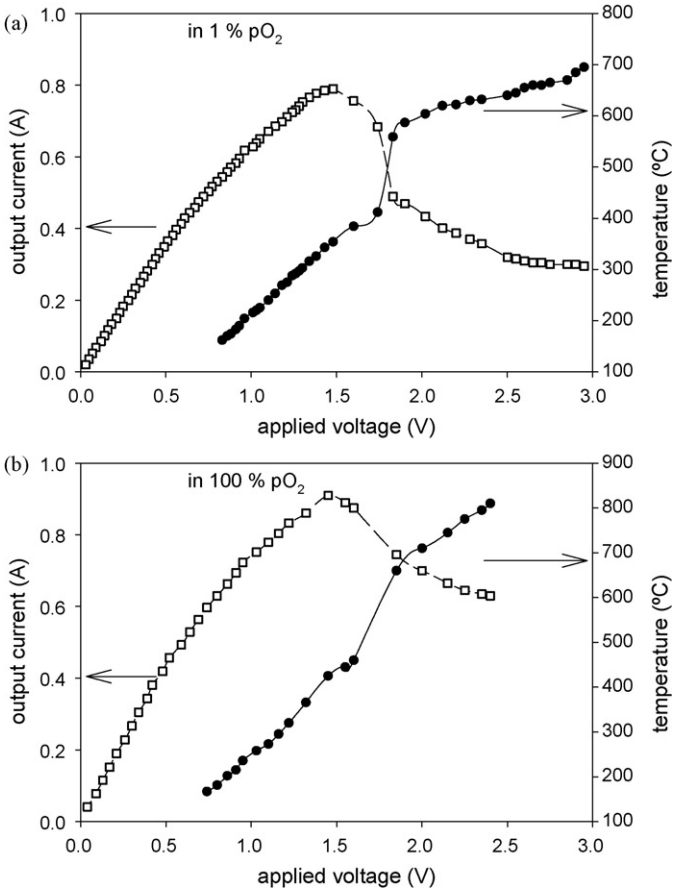

Fig. 2. *I–V* characteristic of the rod and temperature of hot-spot area versus applied voltage across the rod (a) in 1% and (b) in 100% pO_2.

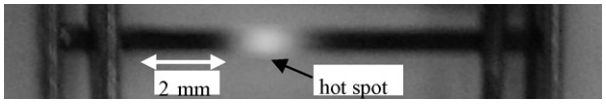

Fig. 3. Appearance of a typical hot spot after applying voltage across the rod in 100% pO_2.

value at applied voltage (V_p) of around 1.5 V followed by a sudden decrease in current with further increase in applied voltage. For the 1% pO_2 case, current appeared to level off for voltage above 2.5 V. Hot-spot temperature measurements for both pO_2, which were simultaneously carried out together with the output current measurements, showed almost linear increase in temperature with voltage below 1.5 V. However, further increase in voltage showed sudden increase in temperature of the hot spots at around 1.8 V. The jump in hot-spot temperature which coincides with the drop in output current beyond the current peak also coincides with appearance of a visible hot spot for both pO_2. Fig. 3 shows appearance of hot spot after applying voltage of 1.9 V across the rod in 100% pO_2. The brightness and temperature of the hot spot increased with increasing voltage and the color changed from dark red to orange. It was also observed that for 100% pO_2 upon reaching a hot-spot temperature of around 650–700 °C, the hot spot began to move to the negative electrode with a velocity of around 2–4 mm/min.

Observation of the gradual decrease in slope of the *I–V* curve between 0.5 V and V_p for Er123 rod (Fig. 2(a) and (b)) in this study is probably due to the accompanying increase in temperature with voltage which acts to increase resistivity of the PTCR material. Observation of the simultaneous jump in hot-spot temperature with drop in output current beyond the current peak (Fig. 2) for both pO_2 is suggested to be related to the direct influence of temperature of the hot spot on resistivity of the rod. It has been reported by Gallagher [10] and Mitberg et al. [11] that for a particular pO_2 environment, there is a drop in equilibrium oxygen content of Y123 samples with increasing temperature of the sample. So in our study, the decrease in current after appearance of the hot spot may be due to increase in resistivity of the hot spot due to reduction in oxygen content as a result of increasing hot-spot temperature. Migration of hot spot towards the negative terminal of the sensor rod is due to diffusion of O^{2-} ions at the hot spot and subsequently its conduction to the positive side of the hot spot as suggested by Takata et al. [3]. This increases the relative resistivity and potential drop in the negative side of the hot spot. As a result, heat generation increases in the negative side and causes the hot spot to move to the negative terminal. In addition, we propose that in equilibrium, net oxygen absorption at the hot spot takes place at the negative side while net oxygen desorption takes place at the positive side of the hot spot due to O^{2-} ion flow towards the positive side. Fig. 4

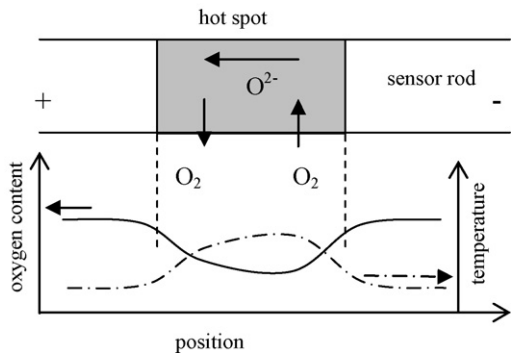

Fig. 4. Schematic representation of the movement of the oxide ion and the net absorption and desorption of the oxygen gas and the oxygen content along the hot spot.

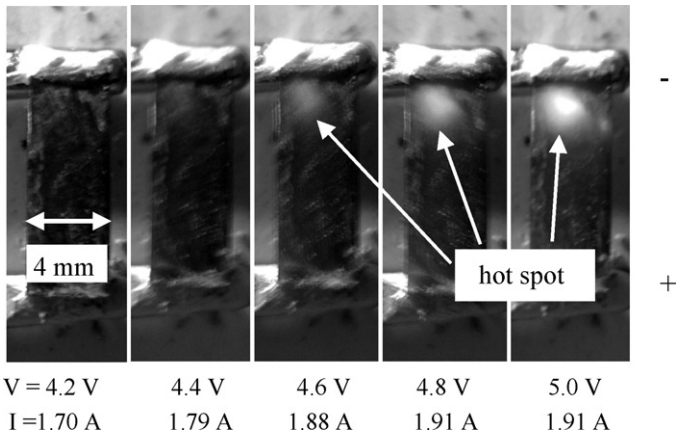

Fig. 5. Sequence photographs of hot spot appearance during increasing in voltage on rectangular shape of sample A.

shows schematic representation of the movement of the oxide ion and the net absorption and desorption of the oxygen gas and the oxygen content along the hot spot.

We also attempted to study the origin of the formation and growth of the hot spot by using a wider Er123 rod shown in Fig. 5. The figure clearly shows hot spot formation starting from a point glow which grows in size and accompanied by increase in visible-color temperature with applied voltage. This observation is evidence that the visible hot-spot formation starts from a single point heating before growing in size. It is suggested that a microstructural defect at the point caused higher potential drop across it and lead to the elevated electrical heating. This is inline with the suggestion by Okamoto et al. [20] that inhomogenuity of resistivity along the sensor rod caused higher potential drop and lead to higher heating and finally glowing of the spot.

In addition, we also observed that when the external applied voltage is switched off and turned back on again, the hot spot reappears at exactly the same location of the previous hot spot before power was turned off. Interestingly, this memory-like effect was observed even after the sensor rod has cooled down to room temperature. It is possible that sudden power off caused the hot spot which was at a particular heated region of the rod to suffer drastic quenching as the temperature decreased to room temperature. This rapid quenching effect produced oxygen deficient region at the hot spot location (Fig. 5) compared to the rest of the rod. This is supported by previous studies on quenching effects on heated RE123 samples which showed large increase in room temperature resistivity due to low oxygen content as a result of rapid cooling [21–24].

Fig. 6(a)–(f) shows output current and hot-spot temperature response with time at different hot-spot temperatures in alternating pO_2 between 1% and 100% for the sensor rod. The stability of output current was clearly observed to improve with increasing hot-spot temperature. For 100% pO_2, no further improvement in output current stability was observed for hot-spot temperature above 745 °C. As such, this study shows that the operating hot-spot temperature of the Er123 sensor rod can be lowered to 745 °C to avoid breakage due to melting at higher temperatures without any compromising current stability. It can also be observed that for starting hot-spot temperature of 655 °C in 1% pO_2 (Fig. 6(a)) the output current in 100% pO_2 increased to 0.9 Å but was not stable and it drops to 0.6 Å in a duration of around 60 s. This may be due to the influence of the hot-spot temperature value which was observed to decrease from 655 °C to 460 °C indicating insufficient Joule heating. The decrease in output current with time is due to the gradual increase in hot-spot temperature which caused resistivity of the PTCR rod to increase. However, a similar temperature drop

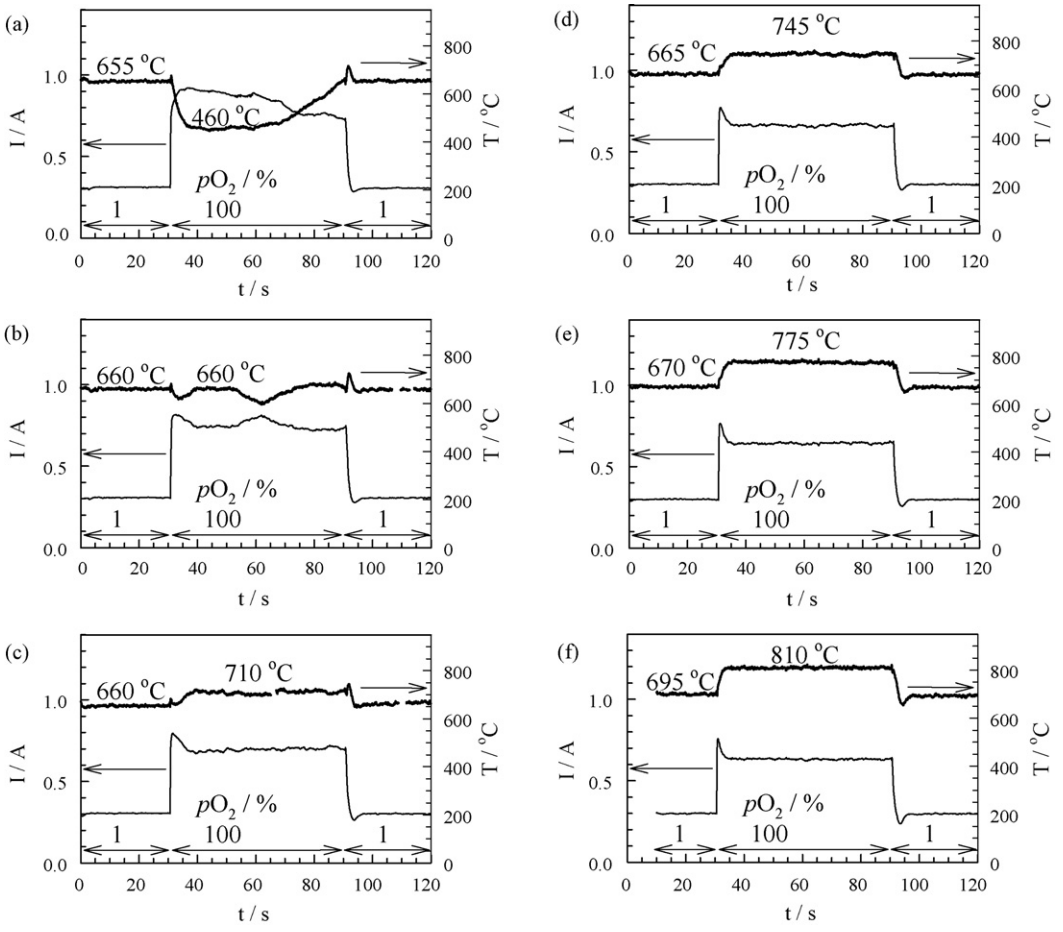

Fig. 6. Output current and hot-spot temperature response with time at different hot-spot temperature in alternating pO_2 between 1% and 100%. The increase in hot-spot temperature from (a) to (f) is due to increase in applied voltage.

of hot-spot temperature in 100% pO_2 was not observed for starting hot-spot temperature of 660 °C in 1% pO_2 (Fig. 6(c)) where output current appeared to have attain stability. As such, from Fig. 6, we suggest that for adequate joule heating to produce stable output current the minimum operating hot-spot temperature for the Er123 sensor rod is 660 °C in 1% pO_2.

Fig. 7(a) shows good repeatability of output current during alternating pO_2 between 1% and 100% whereas Fig. 7(b) shows increase in sensitivity of output current with decreasing pO_2 at the range of pO_2 between 1% and 100%. From Fig. 7(b), the decrease in rate of change with increasing pO_2 indicates that the sensor is more sensitive at low pO_2.

The observed overshoot current in 100% pO_2 for hot-spot temperature of 660 °C and above (Figs. 6 and 7(a)) contributes to increase in output current total response time for the 100% pO_2 detection. The width of overshoot current peaks can be seen to gradually decrease with increasing hot-spot temperature (Fig. 6) and the response time is expected to behave accordingly. In this work we defined total response time, t_{tres} as response time, t_{res} plus overshoot decreasing time, t_{dec}. Response time, t_{res} is defined as the time for output current to increase to maximum, whereas overshoot decreasing time, t_{dec} is defined as the time for 90% reduction in output current from its maximum value. Fig. 8 illustrates the definition of t_{tres}, t_{res} and t_{dec} as defined earlier for an increase in output current with an overshoot. In addition, we also measured total recovery time, t_{trec} for the output current to revert from 100% to 1% pO_2 which is defined as recovery time, t_{rec} plus overshoot increasing time, t_{inc}. Recovery time, t_{rec} is defined as the time for the output current to decrease to minimum value whereas overshoot increasing time, t_{inc} is defined as the time for current to recover to 90% the final value. Table 1 shows t_{res}, t_{dec}, t_{tres}, t_{rec}, t_{inc} and t_{trec} for output current for every change in oxygen partial pressure between 1% and 100% at different hot-spot temperatures.

Table 1
Response time (t_{res}), overshoot decreasing time (t_{dec}), total response time (t_{tres}), recovery time (t_{rec}), overshoot increasing time (t_{inc}) and total recovery time (t_{trec}) of output current for every change in oxygen partial pressure between 1% and 100% at different hot-spot temperature.

Hot-spot temperature (°C)		t_{res} (±0.06 s)	t_{dec} (±0.06 s)	$t_{tres} = t_{res} + t_{dec}$ (±0.06 s)	t_{rec} (±0.06 s)	t_{inc} (±0.06 s)	$t_{trec} = t_{rec} + t_{inc}$ (±0.06 s)
1% pO_2	100% pO_2						
660	710	0.88	4.17	5.05	2.91	2.97	5.88
665	745	0.77	3.40	4.17	2.70	2.36	5.06
670	775	0.61	2.41	3.02	2.97	2.42	5.39
685	795	0.54	2.09	2.63	2.86	2.19	5.05
695	810	0.50	2.80	3.30	2.75	2.09	4.84

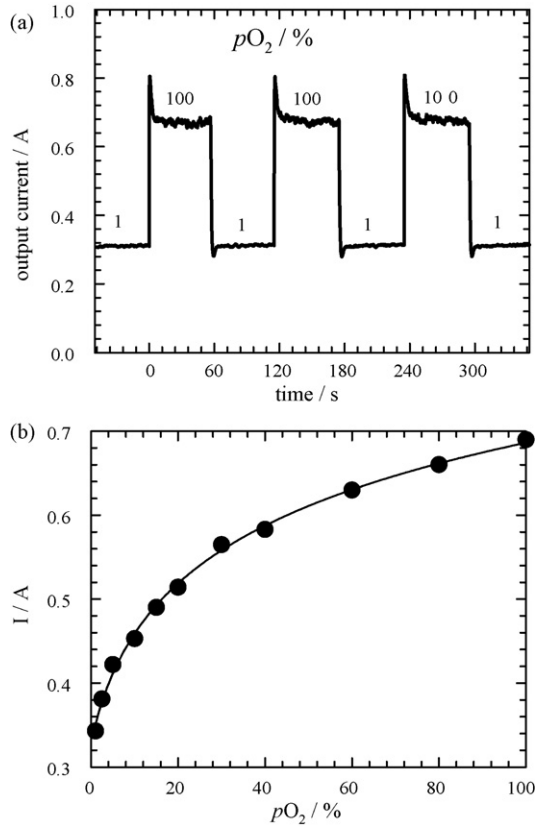

Fig. 7. (a) Repeatability of output current during alternating pO_2 between 1% and 100%, (b) sensitivity of output current between 1% and 100% pO_2.

Table 1 showed that total response time, t_{tres} decreased with increasing hot-spot temperature for the hot-spot temperature up to 685 °C while total recovery time, t_{trec} was less effect by hot-spot temperature. In addition, the hot spot displays slower oxygen desorption (t_{rec}) (2.75–2.91 s) compared to its absorption (t_{res}) (0.50–0.88 s) throughout the temperature range studied. Similar trend was also reported for Y123 material in the absent of the hot spot by Sageev Grader et al. [12] between 320 °C and 750 °C using resistivity measurement and by Hu et al. [13] between 500 °C and 800 °C using thermogavimetry method. We suggest that the model proposed by Lundström [25] where slower sensor recovery may be

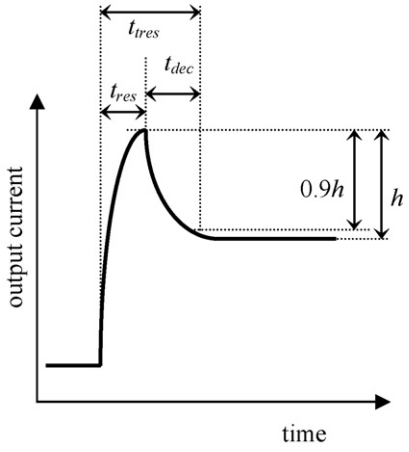

Fig. 8. Sketch diagram to show total response time (t_{tres}), response time (t_{res}) and overshoot decreasing time (t_{dec}) for an increase in output current with overshoot current.

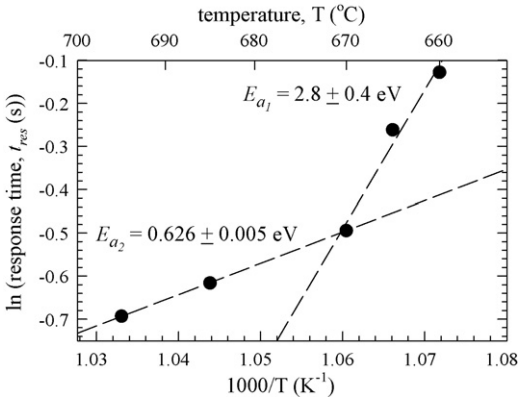

Fig. 9. Arrhenius plot for temperature dependence of the response time. Two possibilities of activation energy (E_a) were estimated using linear fitting.

due to back reaction involving some level of absorption at the surface of the sensor is also applicable to explain the hot-spot response in this study.

The oxygen absorption rate depends on the temperature and can be described by the Arrhenius law behavior for temperature, T dependence of the response time, t_{res} as the latter is inversely proportional to absorption rate [26] where

$$t_{res} = t_o \ \exp\left(\frac{E_a}{k_B T}\right) \quad (2)$$

where t_o is independent of temperature, E_a is the activation energy of ionic migration and k_B is the Boltzmann constant. The plot for ln of t_{res} versus inverse T (Fig. 9) shows two lines with different slopes indicating two different activation energies were involved. From the fitting it was found that the activation energy for hot-spot temperature between 660 °C and 670 °C was 2.78 eV but for higher temperature range between 670 °C and 695 °C the value decreased sharply to 0.63 eV.

Previous works on RE123 materials reported structural transition from orthorhombic to tetragonal (O–T) around 700 °C in 100% pO_2 [11,21,27]. As such, since the change in activation energy was obtained relatively close to the O–T transition temperature, we suggest that the sudden reduction in activation energy shown in Fig. 9 is related to the structural transition. This is supported by previous studies on Y123 where sharp drop in activation energy of oxide ion migration upon reaching tetragonal phase from orthorhombic phase was reported [14,15]. In addition, the O–T transition may also be the reason for the observed movement of the hot spot towards the negative terminal as the hot-spot temperature reaches between 650 °C and 700 °C. The sudden reduction in activation energy is suggested to cause sharp increase in diffusion of O^{2-} ions which triggers the migration. Below 650 °C the material is in the orthorhombic phase where the O^{2-} diffusion is too low to initiate spreading and movement of the hot spot towards the negative terminal due to the higher activation energy.

4. Conclusion

The influence of hot-spot temperature on oxygen sensing response behavior of Er123 rod was studied by simultaneous observation of output current and hot-spot temperature. Stability of the output current was found to improve with increasing hot-spot temperature and the minimum operating hot-spot temperature in 1% pO_2 for stable output current was 660 °C. Sensor response time was found to decrease with increasing temperature with the minimum response time of 0.5 s observed at 695 °C. In addition, we found significant change in activation energy from 2.8 eV to 0.626 eV around 670 °C which is suggested to be related to the change in

structure from orthorhombic to tetragonal taking place around the same temperature. The sudden reduction in activation energy is suggested to cause sharp increase in diffusion of O^{2-} ions which triggers migration of the hot spot to the negative terminal.

Acknowledgement

A.K. Yahya would like to express gratitude and thanks to T. Okamoto for valuable information and discussion leading to this research. This research has been supported by the Malaysian Ministry of Science, Technology and Innovation under e-science grant no. 03-01-01-SF0001.

References

[1] T. Okamoto, M. Takata, Ceram. Int. 30 (2004) 1569–1574.
[2] K. Iihama, Y. Kuroki, T. Okamoto, M. Takata, Curr. Appl. Phys. 9 (2009) S167–S169.
[3] M. Takata, Y. Noguchi, Y. Kurihara, T. Okamoto, B. Huybrechts, Bull. Mater. Sci. 22 (1999) 593–600.
[4] R. Ramamoorthy, P.K. Dutta, S.A. Akbar, J. Mater. Sci. 38 (2003) 4271–4282.
[5] N. Gopal Mandal, Anaesth. Intens. Care Med. 9 (2008) 559–563.
[6] U. Schmid, H. Seidel, G. Mueller, T. Becker, Sens. Actuator B: Chem. 116 (2006) 213–220.
[7] P.R. Warburton, R.S. Sawtelle, A. Watson, A.Q. Wang, Sens. Actuator B: Chem. 72 (2001) 197–203.
[8] T. Eguchi, S. Suda, H. Amasaki, J. Kuwano, Y. Saito, Solid State Ionics 121 (1999) 235–243.
[9] J. Jiang, L. Gao, W. Zhong, S. Meng, B. Yong, Y. Song, X. Wang, C. Bai, Respir. Physiol. Neurobiol. 161 (2008) 160–166.
[10] P.K. Gallagher, Adv. Ceram. Mater. 2 (1987) 632–640.
[11] E.B. Mitberg, M.V. Patrakeev, I.A. Leonidov, A.A. Lakhtin, V.L. Kozhevnikov, K.R. Poeppelmeier, J. Alloys Compd. 274 (1998) 98–102.
[12] G. Sageev Grader, P.K. Gallagher, J. Thomson, M. Gurvitch, Appl. Phys. A: Mater. Sci. Process. 45 (1988) 179–183.
[13] J. Hu, X. Hu, H. Hao, L. Guo, H. Song, D. Yang, Solid State Ionics 176 (2005) 487–494.
[14] S. Tsukui, M. Adachi, R. Oshima, H. Nakajima, F. Toujou, K. Tsukamoto, T. Tabata, Physica C: Supercond. 351 (2001) 357–362.
[15] E. Saiz, J.S. Moya, Mater. Lett. 6 (1988) 369–373.
[16] Y. Tsutai, T. Okamoto, A. Kawamoto, M. Takata, J. Ceram. Soc. Jpn. 112 (1) (2004) S599–S601.
[17] T. Okamoto, M. Takata, J. Ceram. Soc. Jpn. 112 (1) (2004) S567–S571.
[18] T. Okamoto, K. Iihama, M. Takata, Adv. Mater. Res. 11–12 (2006) 137–140.
[19] M. Hassan, A.K. Yahya, K.H. Ku Hamid, Z. Awang, AIP Conf. Proc. 1017 (2008) 295–299.
[20] T. Okamoto, B. Huybrechts, M. Takata, Jpn. J. Appl. Phys. 33 (1994) L1212–L1214.
[21] G. Flor, G. Chiodelli, G. Spinolo, P. Ghigna, Physica C: Supercond. 316 (1999) 13–20.
[22] R. Abd-Shukor, S.S. Lee, M. Yahya, Physica C: Supercond. 243 (1995) 134–138.
[23] S. Tajima, J. Schützmann, S. Miyamoto, Solid State Commun. 95 (1995) 759–764.
[24] J. García López, D.H.A. Blank, H. Rogalla, J. Siejka, Physica C: Supercond. 307 (1998) 298–306.
[25] I. Lundström, Sens. Actuator B: Chem. 35 (1996) 11–19.
[26] A. Helwig, G. Müller, G. Sberveglieri, G. Faglia, Sens. Actuator B: Chem. 130 (2008) 193–199.
[27] G. Chiodelli, I. Wenneker, P. Ghigna, G. Spinolo, G. Flor, M. Ferretti, E. Magnone, Physica C: Supercond. 308 (1998) 257–263.